Computing local stress tensors: a geometric derivation

Lisa Eppler,[1] Martin Hanke,[1] and Thomas Speck[2]

[1] *Institut für Mathematik, Johannes Gutenberg-Universität Mainz, Staudingerweg 7-9, 55128 Mainz, Germany*
[2] *Institut für Physik, Johannes Gutenberg-Universität Mainz, Staudingerweg 7-9, 55128 Mainz, Germany*

We revisit the issue of deriving a local expression for the stress tensor to be used in computer simulations of inhomogeneous systems. We present a novel and transparent geometric derivation in real-space based on volume integrals. This approach allows to make use of Cavalieri's principle in order to explicitly show that one can deform the contour joining two particles while keeping the volume of a body defined by this contour invariant. For inhomogeneous systems along one spatial direction with planar interfaces we recover two previous results for the stress tensor, one associated with cross sections and one due to averaging over a local volume. We illustrate the difference between both expressions in molecular dynamics simulations of a phase-separated Lennard-Jones fluid. The interfacial tension calculated in a finite system is in excellent agreement with previous numerical estimates.

I. INTRODUCTION

Multiscale modeling approaches are concerned with connecting physical processes on different scales and, crucially, different resolutions of the system's degrees of freedom [1–3]. The importance of systematic multiscale approaches for computational sciences is immense since many processes of interest (say, cloud formation) occur over length and time scales that are many orders of magnitude apart from that of their constituents (the water molecules). A paradigmatic example in material science is the connection between the macroscopic stress throughout a piece of material and the microscopic motion of its constituent atoms or molecules (particles in the following). Considering a fixed number of particles in a fixed volume, several routes (via the virial, via the partition function, and via mechanical forces) yield the same expression for the *global* stress tensor [Eq. (10)], which, *inter alia*, allows to calculate bulk elastic moduli of homogeneous model materials in computer simulations.

In continuum mechanics, the Cauchy stress tensor $\boldsymbol{\sigma}$ determines the force $\mathbf{F}$ acting on an imaginary surface S within, or an actual surface of, a body,

$$\mathbf{F} = \boldsymbol{\sigma} \cdot (|S|\mathbf{n}), \tag{1}$$

where $\mathbf{n}$ is the surface normal and $|S|$ the area of S. Conservation of angular momentum implies that $\boldsymbol{\sigma}$ is symmetric in the absence of bulk torques. In an isotropic fluid, the stress tensor reduces to $\boldsymbol{\sigma} = -p\mathbf{1}$ with scalar pressure p. For solids, the number of independent components of the stress tensor is determined by the symmetries of the crystal lattice [4]. In inhomogeneous systems and systems under external load, the stress tensor varies spatially with mechanical equilibrium imposing the force-balance condition $\nabla \cdot \boldsymbol{\sigma} = 0$. Generalizing the expression of the global stress tensor to local volumes that exchange particles with the rest of the system is surprisingly challenging, and a multitude of expressions can be found in the literature which still incites controversy [5, 6]. It is thus desirable to better understand whether and under which conditions unambiguous expressions for a local stress are possible. Such local expressions are required for a number of applications [7], *e.g.*, calculations of the mechanical stress in polymeric thin films [8] and carbon nanopores [9], the line tension of three-phase contact lines [10] and osmotic slip [11], and to study crystal nucleation under shear [12].

Already in 1950, Irving and Kirkwood discussed a local stress tensor [13] (see appendix therein and Sec. II) closely following Eq. (1).[1] They associate an imaginary surface with those particle pairs whose straight connecting line intersects the surface. This result has been generalized by Schofield and Henderson [15]. The expression for the local stress involves a contour integral over the pair distribution function, and the non-uniqueness of this contour–and thus the stress tensor–has been noted early. In particular, Harasima has proposed a non-straight contour in his theory of surface tension [16]. While force balance is obeyed, it has been reported that employing Harasima's contour in spherical coordinates leads to a non-uniform stress tensor in a homogeneous fluid [17, 18], which is of course inconsistent with thermodynamics. For a planar interface, the stress profile of both contours has been compared in Refs. 8, 19.

Another line of studies has followed the idea of an atomic-level stress tensor assigned to each particle, which after coarse-graining enters the evolution equation of the corresponding density [20–22]. Omitting the average of the global stress tensor yields a candidate expression, but one has to decide how to split the force contribution between atoms [23]. Equally distributing one half to each involved atom, however, leads to inconsistencies [24]. In particular, the average normal stress component through a planar interface is non-uniform, violating the mechanical equilibrium condition [8]. Considering momentum flux in Fourier space, Lutsko has derived an expression for an instantaneous stress tensor [25], which after averaging over a local volume takes on a particularly transparent

[1] We point the interested reader to the mathematical work by Walter Noll putting the ideas of Irving and Kirkwood on firmer ground [14].

form involving the fraction of a particle pair's displacement vector inside the volume [26]. More recently, Lion and Allen have obtained a similar result (for the scalar pressure) through a real-space derivation accounting for the particles that enter and leave a small volume [27]. However, all these approaches rely on a straight contour joining two particles.

Here we revisit the problem of deriving a local stress tensor from a purely geometric perspective without appealing to the pair distribution function. Using volume integration of a characteristic function relating particle pairs with a surface, we obtain results for the stress tensor that are manifestly independent of the actual contour connecting the two particles. We recover the standard expression for the global stress and the expression of Walton *et al.* [19] when restricting to a planar cross section of the system. Averaging over a "bin" (an integral of cross sections), our approach confirms the result by Cormier *et al.* [26] specialized to this geometry. It demonstrates that unambiguous expressions for the local stress tensor are possible at least for certain geometries.

II. FROM PAIR FORCES TO STRESS

We consider a system composed of N (point) particles interacting through pairwise forces stemming from the pair potential $u(r)$. Two particles i and j are at positions $\mathbf{r}_i$ and $\mathbf{r}_j$ with displacement vector $\mathbf{r}_{ij} = \mathbf{r}_i - \mathbf{r}_j$ pointing from particle j to particle i [Fig. 1(a)]. The force exerted by particle j onto particle i then is $\mathbf{f}_{ij} = -\nabla_i u(r_{ij}) = -u'(r_{ij})\mathbf{r}_{ij}/r_{ij}$ with $r_{ij} = |\mathbf{r}_{ij}|$ implying Newton's third law $\mathbf{f}_{ji} = -\mathbf{f}_{ij}$.

The stress tensor $\boldsymbol{\sigma} = \boldsymbol{\sigma}_{\mathrm{kin}} + \boldsymbol{\sigma}_{\mathrm{int}}$ can be split into a kinetic contribution $\boldsymbol{\sigma}_{\mathrm{kin}}$ and a contribution $\boldsymbol{\sigma}_{\mathrm{int}}$ due to the interparticle forces. Let Λ be the space of accessible points $\Lambda \subset \mathbb{R}^3$ with fixed volume $|\Lambda|$, and $B \subseteq \Lambda$ a (small) region within Λ. The local kinetic part

$$\boldsymbol{\sigma}_{\mathrm{kin}}(B) = -\frac{1}{|B|}\left\langle \sum_{i=1}^{N} m_i \mathbf{v}_i \mathbf{v}_i \chi_i(B) \right\rangle \tag{2}$$

is unambiguous, with function $\chi_i(B) = 1$ if particle i resides inside B ($\mathbf{r}_i \in B$) and zero otherwise. Here, $\mathbf{v}_i$ is the velocity and m_i the mass of particle i. The brackets $\langle\cdot\rangle$ denote the ensemble average over all particle positions and velocities.

How can we associate a stress tensor $\boldsymbol{\sigma}_{\mathrm{int}}$ with the region B? Obviously, the problem is to find a microscopic prescription how to treat forces that cross the boundary. We start by briefly reviewing the original idea of Irving and Kirkwood [13], which is explored in more detail by Schofield and Henderson [15]. The force on any region B

$$\sum_{i=1}^{N} \langle \mathbf{F}_i \chi_i(B) \rangle = \int_{\partial B} \mathrm{d}^2\mathbf{r}\; \mathbf{n} \cdot \boldsymbol{\sigma}_{\mathrm{int}} = \int_B \mathrm{d}^3\mathbf{r}\; \nabla \cdot \boldsymbol{\sigma}_{\mathrm{int}} \tag{3}$$

is due to the forces exerted by the surrounding material acting onto the surface ∂B with outer normal vector $\mathbf{n}$, cf. Eq. (1). In the second step, we have exploited the divergence theorem to convert the surface integral to a volume integral. Writing $\chi_i(B) = \int_B \mathrm{d}^3\mathbf{r}\; \delta(\mathbf{r} - \mathbf{r}_i)$ with the Dirac δ-distribution, one finds $\sum_i \langle \mathbf{F}_i \delta(\mathbf{r} - \mathbf{r}_i)\rangle = \nabla \cdot \boldsymbol{\sigma}_{\mathrm{int}}$. Using that the total force on each particle is $\mathbf{F}_i = \sum_j \mathbf{f}_{ij}$ leads to

$$\begin{aligned} \sum_i \sum_{j\neq i} \mathbf{f}_{ij} \delta(\mathbf{r} - \mathbf{r}_i) &= \sum_{i<j} \mathbf{f}_{ij} [\delta(\mathbf{r} - \mathbf{r}_i) - \delta(\mathbf{r} - \mathbf{r}_j)] \\ &= \sum_{i<j} \mathbf{f}_{ij} \int_0^1 \mathrm{d}\mathbf{l}_t \cdot \nabla \delta(\mathbf{r} - \mathbf{l}_t). \end{aligned} \tag{4}$$

In the second line we formally exploit the gradient theorem with arbitrary contour $\mathbf{l}_t$ connecting $\mathbf{l}_0 = \mathbf{r}_i$ to $\mathbf{l}_1 = \mathbf{r}_j$, and we exploit translational invariance of the argument to switch to the gradient ∇ with respect to $\mathbf{r}$. Exchanging ∇ with the contour integration then yields the expression

$$\boldsymbol{\sigma}_{\mathrm{int}}(\mathbf{r}) = \left\langle \sum_{i<j} \mathbf{f}_{ij} \int_0^1 \mathrm{d}\mathbf{l}_t \delta(\mathbf{r} - \mathbf{l}_t) \right\rangle. \tag{5}$$

We have thus associated a local stress tensor to a point $\mathbf{r}$ through the contributions of contours passing through an infinitesimal vicinity of $\mathbf{r}$. The choice of the contour joining $\mathbf{r}_i$ with $\mathbf{r}_j$ does not affect the force on the region B, but it allows multiple expressions for pointwise local stress tensors. In their seminal work [13], Irving and Kirkwood have employed a straight contour $\mathbf{l}_t = \mathbf{r}_i - t\mathbf{r}_{ij}$ leading to

$$\boldsymbol{\sigma}^{\mathrm{IK}}_{\mathrm{int}}(\mathbf{r}) = -\left\langle \sum_{i<j} \mathbf{f}_{ij} \mathbf{r}_{ij} \int_0^1 \mathrm{d}t\; \delta(\mathbf{r} - \mathbf{l}_t) \right\rangle. \tag{6}$$

III. GEOMETRIC DERIVATION

A. Basic idea

At this stage one might wonder if it is possible to derive an expression for a local stress tensor that is manifestly independent of the contour joining two particles. Here we show that this is indeed possible exploiting Cavalieri's principle. To this end, let us choose an imaginary planar oriented surface $S \subset \Lambda$ with normal vector $\mathbf{n}$ centered at $\mathbf{r}$ within the system. Our central tool will be the characteristic function $\chi_{ij}(S)$ which is unity if the interactions due to particles i and j contributes to the surface force and zero otherwise (with $\chi_{ji} = \chi_{ij}$ and $\chi_{ii} = 0$). Although the arguably simplest choice is to include pairs if the displacement vector $\mathbf{r}_{ij}$ intersects the surface S, $\chi_{ij}(S)$ is not restricted to a straight line and we will not have to further specify an explicit expression.

With every such surface we associate the force

$$\mathbf{F}(S) = -\left\langle \sum_{(i,j)} \mathbf{f}_{ij} \chi_{ij}(S) \right\rangle \tag{7}$$

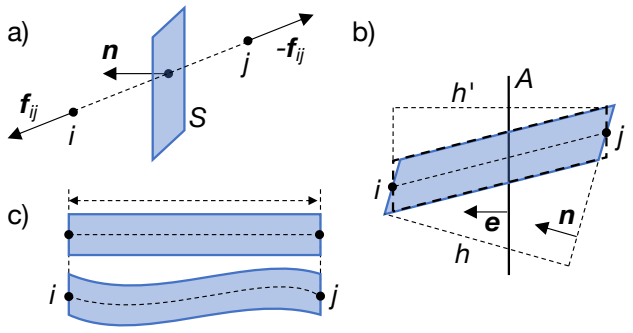

FIG. 1. (a) Sketch of a particle pair (i, j), the bond of which (dashed line) intersects an imaginary surface S (shaded) with normal vector $\mathbf{n}$. Here repulsive forces $\mathbf{f}_{ij}$ and $\mathbf{f}_{ji} = -\mathbf{f}_{ij}$ acting on the particles are shown. (b) Side view onto an oblique prism (shaded) with base area $|S|$ and height $h = |\mathbf{r}_{ij} \cdot \mathbf{n}|$. Rotating base surfaces so that the normal is $\mathbf{e}$ (the normal of the cross section A) yields another prism (dashed outline) with the same volume but height $h' = |\mathbf{r}_{ij} \cdot \mathbf{e}|$. (c) Cavalieri's principle: Deforming the path connecting i and j does not change the volume of the body formed by the intersected surfaces S_t with equal area.

summing over all ordered pairs (i, j) of particle indices. The order is such that $\mathbf{r}_{ij} \cdot \mathbf{n} \geq 0$. Suppose we cut the material along the imaginary surface S and thus cut all bonds connecting two particles contributing to the surface force, pulling the cut open or pressing it together depending on the sign of the force. The crucial step in the following is to identify the force Eq. (7) with the force appearing in Eq. (1), which yields a local expression for the stress tensor $\boldsymbol{\sigma}$. It is not yet useful since it still involves the area of S, which is undetermined. We now show how integrating over the position of S leads to unambiguous expressions for the local stress tensor.

B. Homogeneous systems

We first assume that the material is homogeneous and thus $\boldsymbol{\sigma}$ is constant throughout. Integrating Eq. (1) with the force Eq. (7) over all possible positions $\mathbf{r} \in \Lambda$ of the surface (with fixed normal vector $\mathbf{n}$ and area $|S|$) yields

$$-\left\langle \sum_{(i,j)} \mathbf{f}_{ij} \int_\Lambda \mathrm{d}^3\mathbf{r}\, \chi_{ij}(S) \right\rangle = \boldsymbol{\sigma}_{\mathrm{int}} \cdot \mathbf{n} |S||\Lambda|. \tag{8}$$

The integral

$$\int_\Lambda \mathrm{d}^3\mathbf{r}\, \chi_{ij}(S) = \int_0^h \mathrm{d}t\, |S_t| = |S|h = |S|\mathbf{r}_{ij} \cdot \mathbf{n} \tag{9}$$

calculates the volume of an oblique prism comprising all parallel surfaces S_t that are intersected by the contour connecting i and j, see Fig. 1(b), with equal area $|S_t| = |S|$. In the last step we exploit the order of the indices, which guarantees that the scalar product $h = \mathbf{r}_{ij} \cdot \mathbf{n}$ is non-negative. Note that in Fig. 1(b) a straight line is shown connecting i and j, but Cavalieri's principle [Fig. 1(c)] ensures that a continuous deformation of this line does not change the volume of the body formed by the intersected S_t (under mild conditions, in particular the projected distance h between the base surfaces has to remain the same). Inserting Eq. (9) into Eq. (8) then yields the expression

$$\boldsymbol{\sigma}_{\mathrm{int}} = -\frac{1}{|\Lambda|} \left\langle \sum_{i<j} \mathbf{f}_{ij}\mathbf{r}_{ij} \right\rangle = \frac{1}{|\Lambda|} \left\langle \sum_{i<j} u'(r_{ij}) \frac{\mathbf{r}_{ij}\mathbf{r}_{ij}}{r_{ij}} \right\rangle \tag{10}$$

for the stress in a homogeneous system. It is manifestly symmetric and independent of the area $|S|$. This is the well-known expression for the stress that can be found in textbooks [28].

C. Inhomogeneous systems

We now assume that the system is inhomogeneous in one spatial direction, *e.g.*, because two phases with different densities coexist. We orient the coordinate system so that $\boldsymbol{\sigma} = \boldsymbol{\sigma}(x)$. We consider a cross section $A_x \subset \Lambda$ of the entire system with normal vector $\mathbf{e} = \mathbf{e}_x$. Again integrating over all positions of the surface S but now restricted to the cross section, $\mathbf{r} \in A_x$, we have to consider the integral

$$\int_{A_x} \mathrm{d}^2\mathbf{r}\, \chi_{ij}(S) = |S'|\chi_{ij}(A_x) = \frac{|S||\mathbf{r}_{ij} \cdot \mathbf{n}|}{h'} \chi_{ij}(A_x). \tag{11}$$

Only pairs of particles on both sides of the cross section contribute. The cross section $S' \subset A_x$ of the prism can be calculated as follows [Fig. (1)(b)]: We rotate the base surfaces of the prism to align with the normal vector $\mathbf{e}$. This preserves the volume but changes the height to $h' = |\mathbf{r}_{ij} \cdot \mathbf{e}| = |x_{ij}|$, and the area $|S'|$ is obtained as the previously calculated volume $|S|h$ divided by the height h'. As before, this result is independent of the actual shape of the line connecting i and j thanks to Cavalieri's principle.

Integrating Eq. (7) over all positions $\mathbf{r} \in A_x$, we now obtain

$$-|S| \left\langle \sum_{(i,j)} \mathbf{f}_{ij}\mathbf{r}_{ij} \frac{\chi_{ij}(A_x)}{|x_{ij}|} \right\rangle \cdot \mathbf{n} = \boldsymbol{\sigma}_{\mathrm{int}}(x) \cdot \mathbf{n} |S||A_x|, \tag{12}$$

which yields the symmetric stress tensor

$$\boldsymbol{\sigma}_{\mathrm{int}}(x) = \frac{1}{|A_x|} \left\langle \sum_{i<j} u'(r_{ij}) \frac{\mathbf{r}_{ij}\mathbf{r}_{ij}}{r_{ij}} \frac{\chi_{ij}(A_x)}{|x_{ij}|} \right\rangle \tag{13}$$

associated with the cross section. This is the same expression as derived by Walton *et al.* [19] following Irving and Kirkwood [13], and later reintroduced as "method of planes" [29]. While $\chi_{ij}(A_x)$ still appears explicitly, it is a

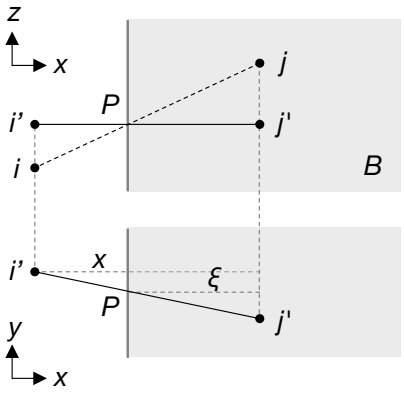

FIG. 2. Sketch of a particle pair (i, j) with particle i residing outside and particle j inside the bin region B (shaded area). Their straight connecting line intersects the cross section at the point P. Top and bottom panel show two projections with i' and j' shifted along z so that $i'j' \perp \partial B$ is perpendicular to the boundary.

simple indicator function selecting all particle pairs that are separated by the cross section but is independent of the actual contour through the cross section.

For practical reasons one is often rather interested in slices $B \subset \Lambda$ with a finite width ℓ ("bins") and volume $|B| = |A_x|\ell$. We first introduce the spatial average

$$\bar{\boldsymbol{\sigma}}_{\rm int}(B) = \frac{1}{|B|}\int_B \mathrm{d}^3\mathbf{r}\ \boldsymbol{\sigma}_{\rm int}(x). \tag{14}$$

We now require the integral

$$\int_B \mathrm{d}^3\mathbf{r}\ \chi_{ij}(A_x) = |A_x|\xi_{ij}(B) \tag{15}$$

with $0 \leqslant \xi_{ij}(B) \leqslant \ell$ the length of the projected separation $|x_{ij}|$ within the bin leading to the average stress

$$\bar{\boldsymbol{\sigma}}_{\rm int}(B) = \frac{1}{|B|}\left\langle \sum_{i<j} u'(r_{ij})\frac{\mathbf{r}_{ij}\mathbf{r}_{ij}}{r_{ij}} l_{ij}(B)\right\rangle \tag{16}$$

within region B. This expression generalizes Eq. (10) to include the ratio $l_{ij}(B) = \xi_{ij}(B)/|x_{ij}|$, which is independent of the contour joining i and j and symmetric, $l_{ji} = l_{ij}$. Eq. (10) is recovered upon extending B to the full system Λ with $l_{ij}(\Lambda) = 1$.

Making use of the intercept theorem, the ratio l_{ij} of the projected distances (onto the normal $\mathbf{e}$) can be expressed also by the particle separation. To this end, note the relations

$$\frac{\xi_{ij}}{|Pj'|} = \frac{|x_{ij}|}{|i'j'|}, \qquad \frac{|i'j'|}{|ij|} = \frac{|Pj'|}{|Pj|}, \tag{17}$$

where i' and j' are the particle positions shifted parallel to the surface so that their displacement vector is perpendicular to the surface with intersection point P (Fig. 2). Rearranging both relations,

$$l_{ij} = \frac{\xi_{ij}}{|x_{ij}|} = \frac{|Pj'|}{|i'j'|} = \frac{|Pj|}{|ij|} \tag{18}$$

is given by the fraction of the separation $|ij| = r_{ij}$ within the volume B. The result Eq. (16) is thus equivalent to the local stress tensor derived by Cormier *et al.* [26] adopted to the present bin geometry.

The same result can already be found from Eq. (5). For particle $\mathbf{r}_j \in B$ inside and $\mathbf{r}_i \notin B$ outside the volume B,

$$\int_0^1 \mathrm{d}\mathbf{l}_t\ \chi_B(\mathbf{r} - \mathbf{l}_t) = \mathbf{r}_P - \mathbf{r}_j \tag{19}$$

with $\mathbf{r}_P$ the intersection point with the surface. For a straight contour we have $\mathbf{r}_P = \mathbf{r}_j + l_{ij}\mathbf{r}_{ij}$, which immediately leads from Eq. (5) to Eq. (16). The advantage of our derivation is that it avoids specifying a contour and makes transparent that the stress tensor Eq. (16) is in fact independent of the contour as long as Cavalieri's principle applies.

IV. NUMERICAL ILLUSTRATION

For an illustration, we perform molecular dynamics simulations of a single-component Lennard-Jones fluid at constant volume V and temperature T with $N = 1105$ particles. The pair potential reads $u(r) = 4\varepsilon(r^{-12} - r^{-6})$, which is cut off and shifted at the distance $r_{\rm c} = 2.5$. The two parameters are the reduced temperature $\tilde{T} = k_{\rm B}T/\varepsilon$ and the global density $\bar{\rho} = N/V$. The integration time step is $\Delta t = 0.005$ in reduced units. We consider equilibrated state points inside the two-phase region, where the homogeneous fluid is unstable and separates into a dense (liquid) and dilute (gas) phase. We employ periodic boundary conditions and a simulation box $2L\times L\times L$ with volume $V = 2L^3$ that is elongated along the x-direction. Due to the periodic boundaries, we obtain two interfaces separating the gas from the liquid phase. Minimizing their area in the elongated box, the interfaces orient so that on average the normal points along the x-axis and the average density profile becomes $\rho(x)$. In the following, the center-of-mass of the system corresponds to $x = 0$.

In Fig. 3, we plot the diagonal components of the stress tensor as a function of x for $\tilde{T} = 0.6$ and $\bar{\rho} = 0.4$. We calculate the two expressions Eq. (16) and Eq. (13) using the same configurations sampled with the molecular dynamics simulations. The system is split into 100 bins with width $\ell = 2L/100$ and area $|A_x| = L^2$. For Eq. (13), the cross section is placed at the center of the bin and we consider all particle pairs that intersect this cross section. As required by mechanical equilibrium, $\sigma_{xx} = \sigma_\perp$ is approximately constant in both cases. Moreover, $\sigma_{yy} = \sigma_{zz} = \sigma_\parallel(x)$ as dictated by the symmetry. We observe that the uncertainties in the dense phase are

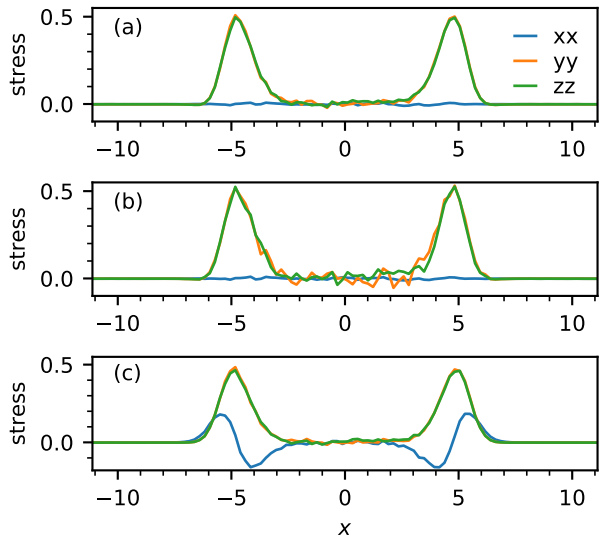

FIG. 3. Diagonal components of the stress tensor $\boldsymbol{\sigma}(x)$ as a function of x for $\tilde{T} = 0.6$ and $\bar{\rho} = 0.4$, whereby $x = 0$ corresponds to the center-of-mass. The same data has been evaluated using for (a) Eq. (16) and for (b) Eq. (13). In (c) we set l_{ij} according to Eq. (20) leading to an unphysical normal stress component σ_{xx}.

much bigger using Eq. (13), while the bin-average method Eq. (16) yields a much smoother profile.

The ad-hoc idea to assign the force evenly to both particles of each pair can be expressed through setting

$$l'_{ij}(B) = \frac{1}{2}[\chi_i(B) + \chi_j(B)] \tag{20}$$

in Eq. (16). The cartesian components of the resulting local stress tensor (again using the same configurations) is plotted in Fig. 3(c). In agreement with previous studies [8, 29], we note that the normal component $\sigma_\perp(x)$ depends on x and is not constant as required by the vanishing divergence of the stress tensor. Such a splitting thus yields unphysical results and is not suitable for calculating the local stress.

While both normal and tangential stress are equal within the two bulk phases, the tangential stress $\sigma_\parallel(x)$ is non-uniform and becomes large within the interfacial region between the two phases. It captures the forces stabilizing the interface, ultimately leading to a macroscopic interfacial tension [32]. This interfacial tension can be calculated from the stress difference [33],

$$\gamma = \int_0^{L/2} \mathrm{d}x\, [\sigma_\parallel(x) - \sigma_\perp]. \tag{21}$$

In Fig. 4, we plot γ as a function of the reduced temperature $\tilde{T}$ employing both methods to calculate the local stress tensor. We also plot results from a previous molecular dynamics study [30] and a Monte Carlo study [31].

Despite the fact that the interfacial tension depends on system size [34], our results are already in excellent agreement although they are obtained in a finite system and not extrapolated to infinite system size. See also Ref. 35 for a more comprehensive discussion of various methods to calculate the interfacial tension.

V. CONCLUSIONS

We have presented a simple derivation for local stress tensors based on the volume integral of a characteristic function. Our result generalizes and supports previous derivations [25–27] for spatially inhomogeneous systems with planar interfaces, yielding an unambiguous local stress tensor for this geometry. Our approach is based on geometric arguments and particularly transparent since it does not require to define a contour joining interacting particles. It will be interesting to study how this geometric approach can be generalized to curved interfaces as relevant for droplets and nucleation phenomena [36]. Moreover, it might shed new insights on the stress in active fluids [37–39].

ACKNOWLEDGMENTS

This research has been enabled by the collaborative research center TRR 146 funded by the Deutsche Forschungsgemeinschaft (DFG, Grant No. 404840447).

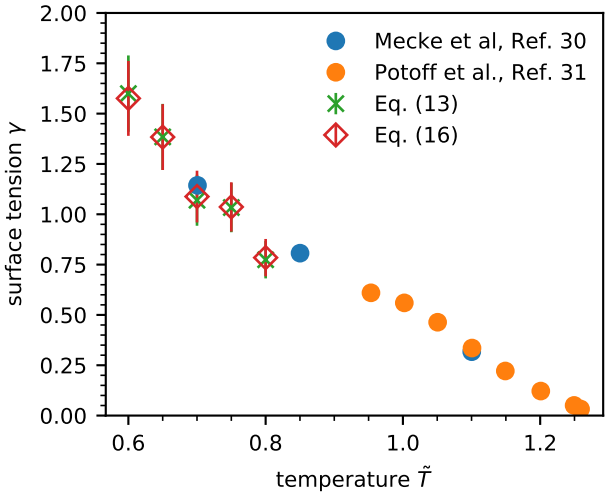

FIG. 4. Interfacial tension γ as function of reduced temperature $\tilde{T} = k_\mathrm{B}T/\varepsilon$. Plotted are the results from Eq. (21) using the stress tensors evaluated using Eq. (13) and Eq. (16). Also plotted are the results from Refs. 30, 31 for comparison.

[1] W. E, *Principles of multiscale modeling* (Cambridge University Press, 2011).

[2] S. Izvekov and G. A. Voth, "Multiscale coarse graining of liquid-state systems," J. Chem. Phys. **123**, 134105 (2005).

[3] C. Peter and K. Kremer, "Multiscale simulation of soft matter systems – from the atomistic to the coarse-grained level and back," Soft Matter **5**, 4357 (2009).

[4] A. K. E.M. Lifshitz and L. Pitaevskii, *Theory of Elasticity* (Elsevier, 1986).

[5] D. van Dijk, Phys. Chem. Chem. Phys. **22**, 9824–9825 (2020).

[6] Y. Long, J. C. Palmer, B. Coasne, K. Shi, M. Śliwińska-Bartkowiak, and K. E. Gubbins, Phys. Chem. Chem. Phys. **22**, 9826–9830 (2020).

[7] T. Nakamura, S. Kawamoto, and W. Shinoda, "Precise calculation of the local pressure tensor in Cartesian and spherical coordinates in LAMMPS," Comput. Phys. Commun. **190**, 120–128 (2015).

[8] F. Varnik, J. Baschnagel, and K. Binder, "Molecular dynamics results on the pressure tensor of polymer films," J. Chem. Phys. **113**, 4444–4453 (2000).

[9] Y. Long, J. C. Palmer, B. Coasne, M. Śliwinska-Bartkowiak, and K. E. Gubbins, "Pressure enhancement in carbon nanopores: a major confinement effect," Phys. Chem. Chem. Phys. **13**, 17163–17170 (2011).

[10] M. Shao, J. Wang, and X. Zhou, "Anisotropy of local stress tensor leads to line tension," Sci. Rep. **5**, 9491 (2015).

[11] R. Ganti, Y. Liu, and D. Frenkel, "Molecular simulation of thermo-osmotic slip," Phys. Rev. Lett. **119**, 038002 (2017).

[12] D. Richard and T. Speck, "Classical nucleation theory for the crystallization kinetics in sheared liquids," Phys. Rev. E **99**, 062801 (2019).

[13] J. H. Irving and J. G. Kirkwood, "The statistical mechanical theory of transport processes. IV. The equations of hydrodynamics," J. Chem. Phys. **18**, 817–829 (1950).

[14] R. B. Lehoucq and A. V. Lilienfeld-Toal, "Translation of Walter Noll's "Derivation of the fundamental equations of continuum thermodynamics from statistical mechanics"," J. Elast. **100**, 5–24 (2010).

[15] P. Schofield and J. R. Henderson, "Statistical mechanics of inhomogeneous fluids," Proc. R. Soc. A **379**, 231–246 (1982).

[16] A. Harasima, "Molecular theory of surface tension," in *Adv. Chem. Phys.*, Vol. 1 (John Wiley & Sons, Inc., 1958) pp. 203–237.

[17] E. M. Blokhuis and D. Bedeaux, "Pressure tensor of a spherical interface," J. Chem. Phys. **97**, 3576–3586 (1992).

[18] B. Hafskjold and T. Ikeshoji, "Microscopic pressure tensor for hard-sphere fluids," Phys. Rev. E **66**, 011203 (2002).

[19] J. P. R. B. Walton, D. J. Tildesley, J. S. Rowlinson, and J. R. Henderson, "The pressure tensor at the planar surface of a liquid," Mol. Phys. **48**, 1357–1368 (1983).

[20] M. Schindler, "A numerical test of stress correlations in fluctuating hydrodynamics," Chem. Phys. **375**, 327–336 (2010).

[21] N. C. Admal and E. Tadmor, "The non-uniqueness of the atomistic stress tensor and its relationship to the generalized Beltrami representation," J. Mech. Phys. Solids **93**, 72–92 (2016).

[22] M. Krüger, A. Solon, V. Démery, C. M. Rohwer, and D. S. Dean, "Stresses in non-equilibrium fluids: Exact formulation and coarse-grained theory," J. Chem. Phys. **148**, 084503 (2018).

[23] Z. S. Basinski, M. S. Duesbery, and R. Taylor, "Influence of shear stress on screw dislocations in a model sodium lattice," Can. J. Phys. **49**, 2160–2180 (1971).

[24] K. S. Cheung and S. Yip, "Atomic-level stress in an inhomogeneous system," J. Appl. Phys. **70**, 5688–5690 (1991).

[25] J. F. Lutsko, "Stress and elastic constants in anisotropic solids: Molecular dynamics techniques," J. Appl. Phys. **64**, 1152–1154 (1988).

[26] J. Cormier, J. M. Rickman, and T. J. Delph, "Stress calculation in atomistic simulations of perfect and imperfect solids," J. Appl. Phys. **89**, 99–104 (2001).

[27] T. W. Lion and R. J. Allen, "Computing the local pressure in molecular dynamics simulations," J. Phys. Condens. Matter **24**, 284133 (2012).

[28] M. P. Allen and D. J. Tildesley, *Computer simulation of liquids* (Oxford University Press, 2017).

[29] B. D. Todd, D. J. Evans, and P. J. Daivis, "Pressure tensor for inhomogeneous fluids," Phys. Rev. E **52**, 1627–1638 (1995).

[30] M. Mecke, J. Winkelmann, and J. Fischer, "Molecular dynamics simulation of the liquid–vapor interface: The Lennard-Jones fluid," J. Chem. Phys. **107**, 9264–9270 (1997).

[31] J. J. Potoff and A. Z. Panagiotopoulos, "Surface tension of the three-dimensional Lennard-Jones fluid from histogram-reweighting Monte Carlo simulations," J. Chem. Phys. **112**, 6411–6415 (2000).

[32] A. Marchand, J. H. Weijs, J. H. Snoeijer, and B. Andreotti, "Why is surface tension a force parallel to the interface?" Am. J. Phys. **79**, 999–1008 (2011).

[33] J. G. Kirkwood and F. P. Buff, "The statistical mechanical theory of surface tension," J. Chem. Phys. **17**, 338–343 (1949).

[34] L.-J. Chen, "Area dependence of the surface tension of a lennard-jones fluid from molecular dynamics simulations," J. Chem. Phys. **103**, 10214–10216 (1995).

[35] K. Binder, B. Block, S. K. Das, P. Virnau, and D. Winter, "Monte Carlo methods for estimating interfacial free energies and line tensions," J. Stat. Phys. **144**, 690–729 (2011).

[36] D. Richard and T. Speck, "Crystallization of hard spheres revisited. II. Thermodynamic modeling, nucleation work, and the surface of tension," J. Chem. Phys. **148**, 224102 (2018).

[37] A. P. Solon, J. Stenhammar, R. Wittkowski, M. Kardar, Y. Kafri, M. E. Cates, and J. Tailleur, "Pressure and phase equilibria in interacting active brownian spheres," Phys. Rev. Lett. **114**, 198301 (2015).

[38] T. Speck and R. L. Jack, "Ideal bulk pressure of active brownian particles," Phys. Rev. E **93**, 062605 (2016).

[39] S. Das, G. Gompper, and R. G. Winkler, "Local stress and pressure in an inhomogeneous system of spherical

active Brownian particles," Sci. Rep. **9**, 6608 (2019).